UC Davis
UC Davis Previously Published Works

Title

Accumulation of 24 nucleotide transgene-derived siRNAs is associated with crinivirus immunity in transgenic plants

Permalink

https://escholarship.org/uc/item/8z22w1fd

Journal

Molecular Plant Pathology, 19(10)

ISSN

1464-6722

Authors

Qiao, Wenjie
Zarzyńska-Nowak, Aleksandra
Nerva, Luca
et al.

Publication Date

2018-10-01

DOI

10.1111/mpp.12695

Peer reviewed

Accumulation of 24 nucleotide transgene-derived siRNAs is associated with crinivirus immunity in transgenic plants

WENJIE QIAO [ID][1], ALEKSANDRA ZARZYŃSKA-NOWAK[2], LUCA NERVA[3,4], YEN-WEN KUO[1] AND BRYCE W. FALK[1,*]

[1]*Department of Plant Pathology, University of California, Davis, CA 95616, USA*
[2]*Department of Virology and Bacteriology, Institute of Plant Protection-National Research Institute, Poznań 60-318, Poland*
[3]*Council for Agricultural Research and Economics – Research Centre for Viticulture and Enology, Conegliano (TV) 00198, Italy*
[4]*Institute for Sustainable Plant Protection, Torino 10135, Italy*

SUMMARY

RNA silencing is a conserved antiviral defence mechanism that has been used to develop robust resistance against plant virus infections. Previous efforts have been made to develop RNA silencing-mediated resistance to criniviruses, yet none have given immunity. In this study, transgenic *Nicotiana benthamiana* plants harbouring a hairpin construct of the *Lettuce infectious yellows virus* (LIYV) RNA-dependent RNA polymerase (RdRp) sequence exhibited immunity to systemic LIYV infection. Deep sequencing analysis was performed to characterize virus-derived small interfering RNAs (vsiRNAs) generated on systemic LIYV infection in non-transgenic *N. benthamiana* plants as well as transgene-derived siRNAs (t-siRNAs) derived from the immune-transgenic plants before and after LIYV inoculation. Interestingly, a similar sequence distribution pattern was obtained with t-siRNAs and vsiRNAs mapped to the transgene region in both immune and susceptible plants, except for a significant increase in t-siRNAs of 24 nucleotides in length, which was consistent with small RNA northern blot results that showed the abundance of t-siRNAs of 21, 22 and 24 nucleotides in length. The accumulated 24-nucleotide sequences have not yet been reported in transgenic plants partially resistant to criniviruses, and thus may indicate their correlation with crinivirus immunity. To further test this hypothesis, we developed transgenic melon (*Cucumis melo*) plants immune to systemic infection of another crinivirus, *Cucurbit yellow stunting disorder virus* (CYSDV). As predicted, the accumulation of 24-nucleotide t-siRNAs was detected in transgenic melon plants by northern blot. Together with our findings and previous studies on crinivirus resistance, we propose that the accumulation of 24-nucleotide t-siRNAs is associated with crinivirus immunity in transgenic plants.

Keywords: *Crinivirus*, *Cucurbit yellow stunting disorder virus*, deep sequencing, immunity, *Lettuce infectious yellows virus*, RNA silencing.

Correspondence: Email: bwfalk@ucdavis.edu

INTRODUCTION

RNA silencing is a natural gene regulation and defence mechanism against aberrant RNA molecules, mediated by small RNAs through DNA methylation at the transcriptional level or mRNA interference at the post-transcriptional level (Pumplin and Voinnet, 2013). Plant viruses are strong inducers as well as targets of RNA silencing (Pantaleo *et al.*, 2010). Virus-derived small interfering RNAs (vsiRNAs), generated on virus infection, are processed from viral double-stranded RNAs (dsRNAs), formed during virus replication and transcription, and from extensive secondary structures of viral RNA, which serve as substrates for Dicer-like ribonucleases (DCLs) to be cleaved into 21–24-nucleotide (nt) vsiRNA duplexes. Secondary vsiRNAs can also be produced via the amplification of dsRNA by host-encoded RNA-dependent RNA polymerases (RdRps) (Wassenegger and Krczal, 2006). The vsiRNAs are then loaded into Argonaute (AGO) proteins to form RNA-induced silencing complexes (RISCs) to target viral and host RNAs by sequence complementarity (Borges and Martienssen, 2015; Ding and Voinnet, 2007). In the model plant *Arabidopsis thaliana*, DCL4, DCL2 and DCL3 confer antiviral defences by catalysing the formation of 21-, 22- and 24-nt vsiRNAs, respectively (Ding, 2010; Ding and Voinnet, 2007). DCL4 and DCL2 confer efficient antiviral defence in plants and exhibit functional redundancy or cooperative interactions (Deleris *et al.*, 2006; Garcia-Ruiz *et al.*, 2010). The 21- and 22-nt vsiRNAs are generally the most predominant classes in virus-infected host plants (Garcia-Ruiz *et al.*, 2010; Ogwok *et al.*, 2016). DCL3 produces 24-nt siRNAs inducing the transcriptional repression of transposons and chromatin modifications of transgenes and repeated sequences in plants, and may enhance the antiviral defences mediated by DCL4 and DCL2 (Diaz-Pendon *et al.*, 2007; Matzke and Birchler, 2005). So far, higher plants are known to encode at least 10 AGO genes, although the specific contribution of AGOs in antiviral silencing is largely unknown for most plant species (Odokonyero *et al.*, 2017). In *Arabidopsis*, multiple AGO proteins have been identified as participating in antiviral defences (Carbonell and Carrington, 2015), and the sorting of vsiRNAs into specific *Arabidopsis* AGO complexes is preferentially directed by their 5′-terminal nucleotide (Mi *et al.*, 2008).

Lettuce infectious yellows virus (LIYV) is a type member in the genus *Crinivirus* that includes the whitefly-transmitted members of the family *Closteroviridae* (Tzanetakis *et al.*, 2013). Criniviruses are characterized by their large bipartite genomes of positive-sense, single-stranded RNA of approximately 15–18 kb in total (Kiss *et al.*, 2013; Tzanetakis *et al.*, 2013). RNA1 encodes proteins that are predominantly associated with replication: the 5′-terminal replicative module consisting of open reading frames (ORFs) 1a and 1b that code for the conserved domains of papain-like cysteine proteinase (PRO), methyltransferase (MTR), helicase (HEL) and RdRp (Yeh *et al.*, 2000). RNA2 encodes several proteins functioning in other aspects, such as virus encapsidation, movement and vector transmission (Stewart *et al.*, 2010; Tian *et al.*, 1999). Criniviruses have emerged as major problems for agriculture by causing severe diseases in various currently important crops worldwide and lead to considerable economic losses. *Cucurbit yellow stunting disorder virus* (CYSDV), for example, has become a significant production threat throughout cucurbit production regions worldwide since its successful spread from the Middle East. *Sweet potato chlorotic stunt virus* (SPCSV) is another notorious crinivirus threatening sweet potato production, one of the most important staple foods available today in sub-Saharan Africa (Tzanetakis *et al.*, 2013).

The management of plant diseases caused by various criniviruses has been problematic. Strategies such as insecticide application against whitefly vectors, preventative cultural practices and the use of genetically resistant cultivars have only provided limited success, together with concerns such as environmental pollution, high costs and long, laborious testing periods (Abrahamian and Abou-Jawdah, 2014; Aguilar *et al.*, 2006; Marco *et al.*, 2003; McCreight and Wintermantel, 2011; Okuda *et al.*, 2013; Park *et al.*, 2006). RNA silencing-based resistance is a powerful tool that has been used to engineer virus-resistant plants for nearly 30 years (Prins *et al.*, 2008; Simón-Mateo and García, 2011). Plants transformed with a hairpin construct consisting of an inverted repeat sequence from the viral genome are often able to induce RNA silencing and confer viral resistance (Helliwell and Waterhouse, 2005; Smith *et al.*, 2000). Reports on the use of RNA silencing to develop resistance amongst criniviruses have so far been limited to attempts with SPCSV. Sweet potato (*Ipomoea batatas* L.) plants transformed with a gene fragment of the SPCSV coat protein (CP) and RdRp have been tested; both displayed some degree of resistance in the form of delayed, attenuated symptoms and reduced virus titre, but none have given immunity (Kreuze *et al.*, 2008; Sivparsad and Gubba, 2014).

Our laboratory has been focusing on the development of transgenic plants immune to LIYV. Transgenic lettuce (*Lactuca sativa*) and *Nicotiana benthamiana* plants transformed with sequences from several ORFs on LIYV RNA2 have been developed, but failed to give LIYV immunity (Kiss, 2013). More recently, we have tried new approaches to generate four transgenic *N. benthamiana* lines comprising sequence fragments from the LIYV replicase coding region of PRO, MTR, HEL and RdRp on RNA1. Among them, only that harbouring an 801-nt fragment of the RdRp gene showed consistent immunity in all tests, as revealed by the lack of symptoms and failure to detect LIYV in these plants. By contrast, the MTR transgene appeared to be lethal to *N. benthamiana* plants, systemic LIYV infections were seen in HEL-transgenic plants and, although the T_0 plants showed immunity, later generations of PRO-transgenic plants did not (Kiss, 2013). In this study, the RdRp-transgenic *N. benthamiana* plants were further characterized with regard to their immunity to systemic LIYV infection. By using deep sequencing analysis to compare transgene-derived siRNAs (t-siRNAs) from LIYV immune plants with vsiRNAs from LIYV-infected non-transgenic plants, we found that siRNAs which mapped to the RdRp transgene region showed a similar pattern in both LIYV-infected and transgenic immune plants, except that a greater proportion of 24-nt siRNAs was seen in transgenic plants. The accumulation of 24-nt t-siRNAs was also found in CYSDV immune-transgenic melon plants, but not in other transgenic plants partially resistant to criniviruses, indicating their association with crinivirus immunity.

RESULTS

Molecular characterization of RdRp-transgenic *N. benthamiana* plants and their immunity to LIYV infection

Transgenic *N. benthamiana* plants were generated through *Agrobacterium tumefaciens*-mediated transformation with a vector constructed by cloning an 801-nt RdRp gene fragment into the hairpin configuration of the binary vector pCB2004B using the Gateway cloning system (Fig. 1A) (Kiss, 2013; Lei *et al.*, 2007). Plants of the T_1 and T_2 generations screened on selective culture medium and which tested positive by polymerase chain reaction (PCR) were used for further study. Transgene expression was examined in transformed *N. benthamiana* plants by reverse transcription-polymerase chain reaction (RT-PCR). Transcripts of transgenic RNA were detected only in transgenic plants with primers specific to the transgene sequences (Fig. 1B). Northern blot hybridization was used to test for the presence of t-siRNAs. Hybridization showed t-siRNAs of 21, 22 and 24 nt in RdRp-transgenic *N. benthamiana* plants, but not in healthy, non-transgenic controls (Fig. 1C).

To test LIYV resistance, both transgenic and non-transgenic *N. benthamiana* plants were challenged with LIYV by agroinoculation and *Bemisia tabaci* transmission at the four- to six-leaf stages. In three independent trials, 20 of 25 agroinoculated and 26 of 26 *B. tabaci*-inoculated non-transgenic plants showed typical LIYV symptoms, including interveinal yellowing symptoms on older
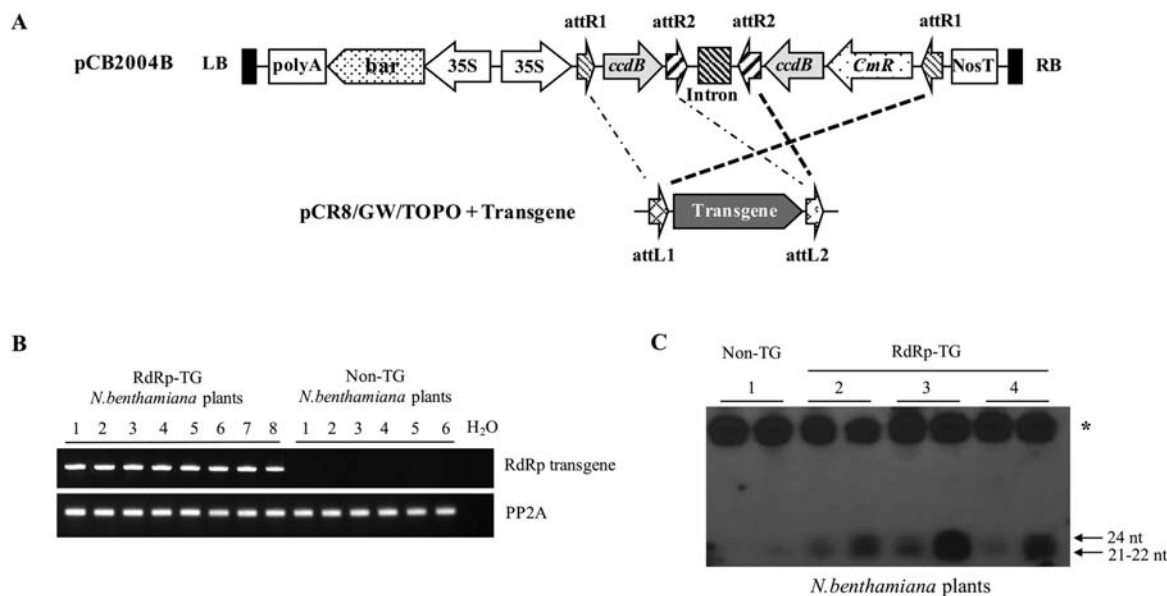
Fig. 1 Molecular characterization of transgenic *Nicotiana benthamiana* plants. (A) Schematic representation of the binary vector pCB2004B construct within the left (LB) and right (RB) borders that was used for plant transformation. Transgenes were delivered from the TA-cloning vector pCR™8/GW/TOPO into pCB2004B through the Gateway cloning system; the resulting T-DNA contains the transgene in antisense and sense orientations separated by an intron sequence, under the control of the 35S promoter (35S) and the nos poly-A terminator (NosT). The bar selection gene is parallel under the control of another 35S-poly-A terminator. *CmR*, chloramphenicol resistance gene; *ccd*B, gene for counter selection in regular cloning host; attR1/2 and attL1/2, recombination sites of λ phage excisionase. (B) Transgene expression in transgenic *N. benthamiana* (RdRp-TG) plants was examined by reverse transcription-polymerase chain reaction (RT-PCR). Non-transgenic (Non-TG) plants were used as controls. RT-PCR was performed using primers corresponding to the RNA-dependent RNA polymerase (RdRp) transgenes. The same RNA samples were used to amplify the PP2A (protein phosphatase) as reference control for *N. benthamiana* plants. The numbers above the gel represent samples from different plants. (C) Northern blot analysis of the transgene sequence-derived small RNAs in transgenic and non-transgenic *N. benthamiana* plants. Sample 1, non-transgenic plant before (left) and after (right) *Lettuce infectious yellows virus* (LIYV) infection; samples 2–4, transgenic plants before (left) and after (right) LIYV inoculation. Each sample represents one plant. A cross-reacting band (asterisk) was used as a loading control. nt, nucleotide.

leaves at 3 weeks post-inoculation (wpi). In contrast, all the T₂ RdRp-transgenic *N. benthamiana* plants tested (90/90) did not exhibit any symptoms and displayed resistance to LIYV infection (Fig. 2A; Table 1). The five agroinoculated non-transgenic plants that did not show systemic infection are probably the result of the efficiency of LIYV agroinoculation, as reported by Wang *et al.* (2009). LIYV RNA was successfully amplified with total RNAs extracted from systemically infected non-transgenic *N. benthamiana* plants by RT-PCR using primers specific to the CP sequence at 4 wpi, but not from transgenic plants (Fig. 2B). These results therefore show the immunity of RdRp-transgenic *N. benthamiana* plants to systemic LIYV infection.

Deep sequencing of small RNAs from non-transgenic and transgenic *N. benthamiana* plants

To better characterize small RNA populations and obtain insight into the mechanisms of RNA-based antiviral immunity and counter-defence in crinivirus–host interactions, 12 libraries were constructed with small RNAs isolated from the same non-

transgenic and RdRp-transgenic *N. benthamiana* plants before and 3 weeks after LIYV inoculation; three plants were randomly chosen for each. The sequencing was performed with an Illumina Hiseq4000 system and each generated 6–11 million clean reads ranging from 18 to 30 nt (Table 2). Three biological replicates of each set were analysed individually and showed very similar patterns. The results described below were the averages generated from three biological replicates. Detailed data analysis on individual libraries can be found in Table S1 (see Supporting Information). The size distribution of the total small RNAs within these different sets was similar, dominated by 24 nt in length, representing around 50% in total (Fig. 3A). Total reads from the non-transgenic and transgenic *N. benthamiana* plants were aligned to the LIYV genome (Accession: NC_003617.1, NC_003618.1) and the RdRp transgene sequence using Bowtie2 in the Galaxy platform; no mismatches or gaps were allowed (Langmead and Salzberg, 2012). 525 778 vsiRNA reads were identified in LIYV-infected non-transgenic *N. benthamiana* plants, accounting for 5.73% of the total, whereas only 40 reads, on average, matched to the LIYV genome in the healthy control (Table 2). In transgenic
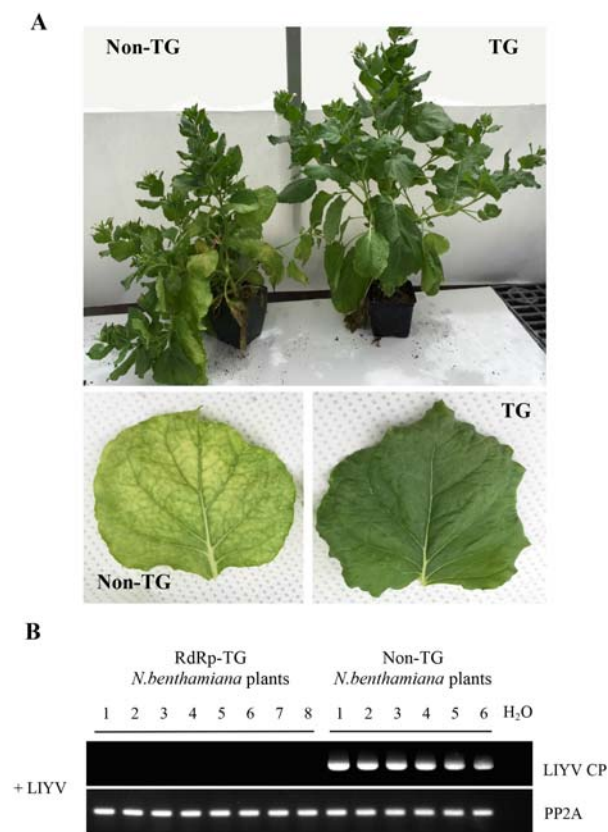
Fig. 2 Examination of *Lettuce infectious yellows virus* (LIYV) resistance of *Nicotiana benthamiana* transgenic plants. (A) Responses of non-transgenic (Non-TG) and transgenic (TG) *N. benthamiana* plants to LIYV inoculation. Symptoms were observed at 4 weeks post-inoculation. (B) Reverse transcription-polymerase chain reaction (RT-PCR) was performed using total RNA extracted from TG and non-TG *N. benthamiana* plants that had been inoculated with LIYV; primers corresponding to the coat protein (CP) were used. The same RNA samples were used to amplify the PP2A (protein phosphatase) gene as reference control for *N. benthamiana* plants. Numbers above the gel represent samples from different plants.

N. benthamiana plants before and after LIYV inoculation, almost all reads that mapped to the LIYV genome were generated from the RdRp transgene sequence, accounting for 0.26% and 0.47%, respectively, of the total small RNA reads; only 19 and 41 reads,

on average, respectively, were counted as mapped to other LIYV genomic regions, similar to the amount of reads detected in the healthy non-transgenic control (Table 2). The sequencing results thus verified the accumulation of t-siRNAs from the hairpin construct, and the immunity of these plants to LIYV infection. In comparison, vsiRNA reads from LIYV-infected non-transgenic plants referring to the RdRp transgene region accounted for 0.14% of the total (Table 2).

Characterization of vsiRNAs in LIYV-infected, non-transgenic *N. benthamiana* plants

The accumulation of vsiRNAs indicates the activation of the RNAi machinery and antiviral defence of the host on viral infection, and may help to decipher the mechanisms and components involved in their biogenesis and function. Size distribution analysis showed that the vsiRNAs produced on LIYV infection were predominantly of 21 and 22 nt in length, representing 23% and 29% of the total, respectively (Fig. 3B), suggesting that DCL4 and DCL2 may be the predominant Dicer ribonucleases involved in vsiRNA biogenesis.

Further analyses were performed for canonical small RNAs ranging from 21 to 24 nt derived from the viral sequences (Aliyari *et al.*, 2008; Borges and Martienssen, 2015). The distribution of 21–24-nt vsiRNA reads along the genomic RNAs of LIYV was examined to explore their origin. The single-nucleotide resolution maps indicated that vsiRNAs from both polarities were almost continuously, but heterogeneously, distributed throughout the LIYV genome (Fig. 4A); more than three times more vsiRNA reads were found to be derived from LIYV RNA2 than from LIYV RNA1 (Fig. 4B). Almost equivalent amounts of sense (54%) and antisense (46%) vsiRNAs suggested that vsiRNAs were derived from both sense and antisense LIYV RNA strands to a similar extent (Fig. 4C).

It has been shown in *A. thaliana* that the selective loading of small RNAs into specific AGOs is determined by the 5′-terminal nucleotide (Brodersen *et al.*, 2008). To determine the potential interactions between vsiRNAs with distinct AGO complexes, the relative abundance of vsiRNAs according to their 5′-terminal nucleotides was analysed. For the vsiRNAs of 21–24 nt, U was the most abundant nucleotide at the 5′-end, followed by A, whereas G was the least abundant (Fig. 4D). These results suggest that vsiRNAs are potentially loaded into diverse AGO-containing complexes, with most preferentially loaded into AGO1 and AGO2, which showed a preference for U and A (Mi *et al.*, 2008).

Characterization of t-siRNAs in RdRp-transgenic *N. benthamiana* plants

To understand the significance of t-siRNAs in LIYV resistance, t-siRNAs generated from the RdRp transgene of transgenic *N. ben-thamiana* plants after LIYV inoculation were characterized and compared with vsiRNAs that mapped to the same region (RdRp-

Table 1 Numbers of non-transgenic (Non-TG) and RNA-dependent RNA polymerase (RdRp)-transgenic (RdRp-TG) *N. benthamiana* plants showing viral symptoms recorded at 4 weeks post-inoculation.

LIYV challenge	Non-TG *N. benthamiana*		RdRp-TG *N. benthamiana*	
	Agroinoculation	Whitefly	Agroinoculation	Whitefly
Trial 1	7/9	9/9	0/16	0/12
Trial 2	5/7	8/8	0/16	0/18
Trial 3	8/9	9/9	0/14	0/14
Total	20/25	26/26	0/46	0/44

Table 2 Twelve libraries constructed with small RNAs from non-transgenic (Non-TG) and RNA-dependent RNA polymerase (RdRp)-transgenic (RdRp-TG) *Nicotiana benthamiana* plants before and after *Lettuce infectious yellows virus* (LIYV) inoculation, including four treatments and three biological replicates each.

Library	*N. benthamiana*	LIYV inoculation	Clean reads	18–30-nt reads (total reads)	Reads on LIYV (percentage of total)	Reads on RdRp (percentage of total)
1	Non-TG-1	Before	10 072 945	9 974 564	37 (0.00%)	0
2	Non-TG-2	Before	7 643 694	7 597 973	29 (0.00%)	0
3	Non-TG-3	Before	10 791 479	10 738 247	52 (0.00%)	0
4	Non-TG-1	After	9 006 404	8 963 149	439 438 (4.90%)	10 016 (0.11%)
5	Non-TG-2	After	10 502 138	10 357 458	481 696 (4.65%)	11 436 (0.11%)
6	Non-TG-3	After	8 641 889	8 594 701	656 200 (7.63%)	16 490 (0.19%)
7	RdRp-TG-1	Before	10 751 736	10 716 583	23 802 (0.22%)	23 785 (0.22%)
8	RdRp-TG-2	Before	6 725 887	6 615 436	25 839 (0.39%)	25 830 (0.39%)
9	RdRp-TG-3	Before	10 465 709	10 452 946	17 733 (0.17%)	17 712 (0.17%)
10	RdRp-TG-1	After	8 632 939	8 615 976	43 732 (0.51%)	43 691 (0.51%)
11	RdRp-TG-2	After	9 424 712	9 401 315	44 214 (0.47%)	44 189 (0.47%)
12	RdRp-TG-3	After	9 688 046	9 651 174	42 419 (0.44%)	42 360 (0.44%)

Clean reads, reads obtained from BGI after adapter trimming and cleaning; 18–30-nt reads, total small interfering RNA (siRNA) reads analysed; Reads on LIYV, number of reads aligned to the LIYV genome; Reads on RdRp, number of reads aligned to the RdRp transgene sequence; the percentage of the aligned reads of the total 18–30-nt reads is listed.

vsiRNAs) in LIYV-infected, non-transgenic *N. benthamiana* plants at the same stage. The 21–24-nt t-siRNAs were sorted according to sequence and size. The sequence distribution profile of t-siRNAs on the RdRp transgene segment was constructed, showing a pattern of t-siRNAs that accumulated in several hotspot regions (peaks) located throughout the transgene sequence. Interestingly, a very similar profile showing peaks in the same locations was observed with RdRp-vsiRNAs, although the relative numbers of reads in each peak varied (Fig. 5A). The fact that similar t-siRNA and RdRp-vsiRNA distribution patterns were observed indicates that a sequence bias in the t-siRNA population depends on a nucleotide sequence preference.

The size distribution of t-siRNAs showed that lengths of 21 and 22 nt made up the most abundant size classes in both

orientations, each representing 24% of the total t-siRNAs, followed by 17% of DCL3-dependent 24-nt reads (Fig. 5B). Similarly, the 21- and 22-nt classes accounted for a majority of the RdRp-vsiRNAs (25% and 30%, respectively). However, despite the similar distribution patterns of t-siRNAs and RdRp-vsiRNAs, a much lower percentage of the 24-nt class ($\sim$3%) was observed in the latter (Fig. 5B). The deep sequencing data were supported by the results of northern blot hybridization, which showed 21- and 22-nt RdRp-vsiRNAs in LIYV-infected non-transgenic *N. benthamiana* plants, whereas t-siRNAs of 21, 22 and 24 nt accumulated in transgenic *N. benthamiana* plants (Fig. 1C). In contrast, northern blot analysis in previous studies on transgenic plants that were susceptible or partially resistant to crinivirus infection showed the accumulation of only 21- and 22-nt t-siRNAs (Kiss, 2013; Kreuze
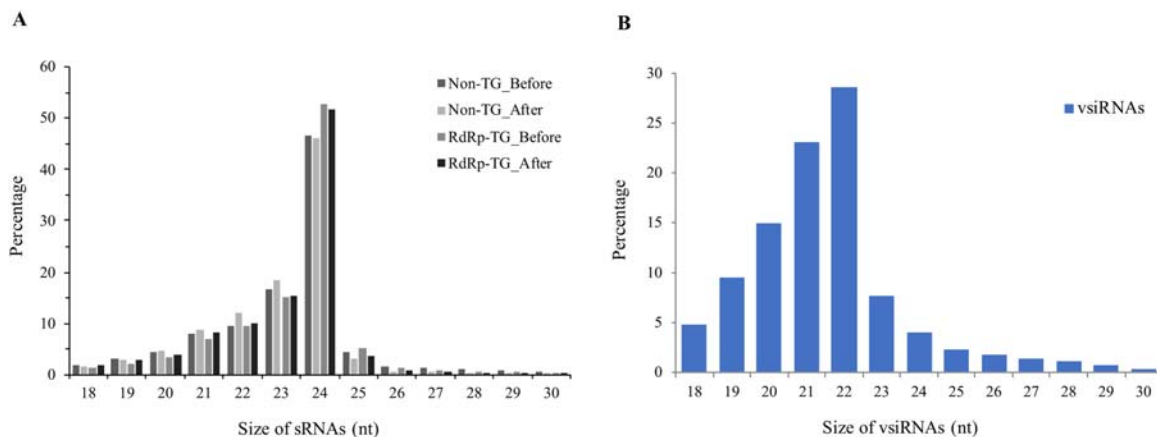

Fig. 3 Size distribution of the 18–30-nucleotide total small RNAs from non-transgenic (Non-TG) and RNA-dependent RNA polymerase (RdRp)-transgenic (RdRp-TG) *Nicotiana benthamiana* plants before and after *Lettuce infectious yellows virus* (LIYV) inoculation (A) and virus-derived small interfering RNAs (vsiRNAs) from LIYV-infected non-transgenic *N. benthamiana* plants (B).
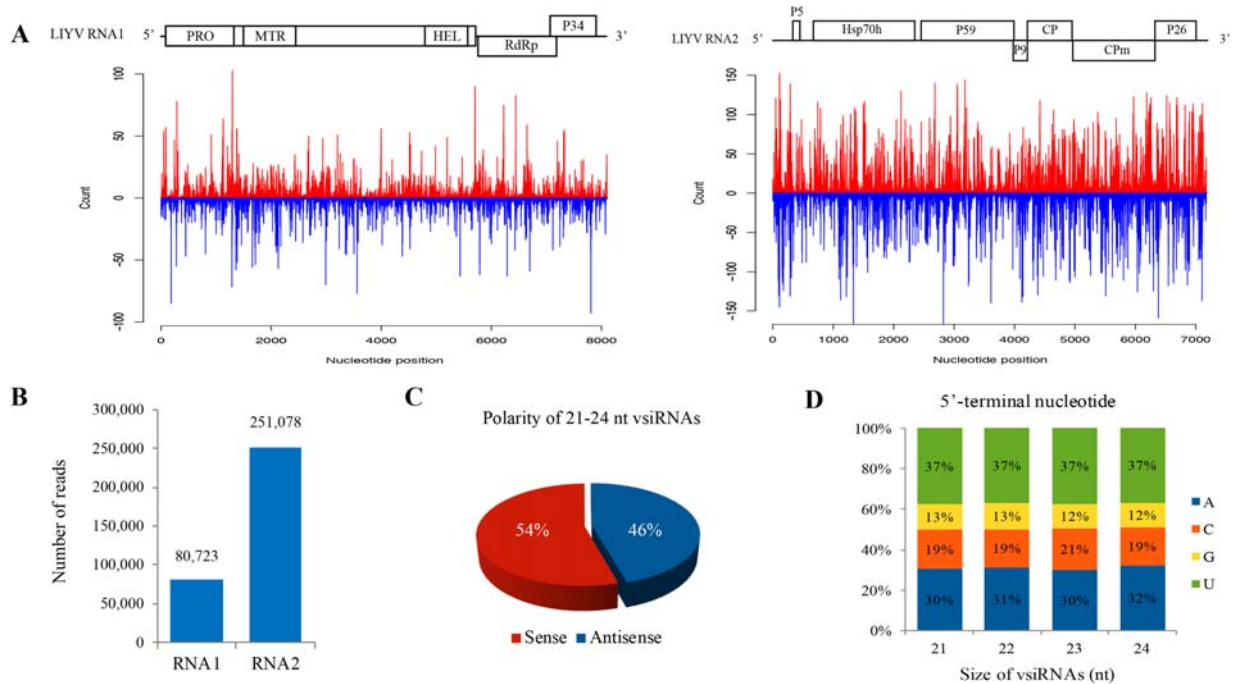
Fig. 4 Profile of 21–24-nucleotide (nt) virus-derived small interfering RNAs (vsiRNAs) derived from *Lettuce infectious yellows virus* (LIYV)-infected non-transgenic *Nicotiana benthamiana* plants. (A) Single-nucleotide resolution maps of vsiRNAs along the LIYV genomic RNAs in both positive (red) and negative (blue) polarity. Schematic diagram of the LIYV genomic RNAs positioned above proportionally. Distribution maps shown are generated from library 4 (Non-TG-1); two other biological replicates (Non-TG-1) displayed a similar pattern and can be found in Fig. S1 (see Supporting Information). CP, coat protein; HEL, helicase; MTR, methyltransferase; PRO, papain-like cysteine proteinase; RdRp, RNA-dependent RNA polymerase. (B) Number of reads on LIYV RNA1 and RNA2. Total number is shown above the bar. (C) Accumulation of sense and antisense vsiRNAs. Percentage is shown within the pie graph. (D) Relative frequency of 5′-terminal nucleotides in 21–24-nt vsiRNAs.

et al., 2008). We hypothesized that the elevated levels of 24-nt t-siRNAs in our transgenic plants may be associated with crinivirus immunity.

To explore the origin of t-siRNAs, the polarity distribution of t-siRNAs was further characterized. Almost equivalent amounts of sense and antisense forms were counted for both t-siRNAs and RdRp-vsiRNAs, although the antisense (52%) t-siRNA amounts were slightly greater that those of the sense (48%) orientation, whereas, for RdRp-vsiRNAs, slightly more reads were counted in the sense (52%) orientation (Fig. 5B). The 5′-terminal nucleotides were compared for the 21–24-nt t-siRNAs and RdRp-vsiRNAs. The ratio of the four nucleotides for t-siRNAs and RdRp-vsiRNAs in the same size class showed no statistically significant difference when analysed with the *t*-test. U was the most common 5′ nucleotide, followed by A, in all four sizes of t-siRNAs and RdRp-vsiRNAs (Fig. 5C).

Furthermore, we also characterized the t-siRNA populations of transgenic plants before and after viral inoculation. The analysis showed highly similar distribution patterns between the t-siRNAs of transgenic plants before and after viral inoculation (Fig. S2, see Supporting Information), although the number of t-siRNA reads for each size class between 21 and 24 nt in transgenic plants at 3

wpi was about two-fold greater compared with transgenic plants before viral inoculation (Table S1).

Accumulation of 24-nt t-siRNAs in CYSDV immune-transgenic melon (*Cucumis melo*) plants

To test our hypothesis that the accumulation of 24-nt t-siRNAs is associated with crinivirus immunity in transgenic plants, we developed transgenic melon (*C. melo*) plants for another crinivirus, CYSDV, transformed with a hairpin construct of the CYSDV PRO gene. Transgenic melon plants were screened as described above for transgenic *N. benthamiana* plants by selective medium and PCR. Transcripts of the transgene RNA were confirmed using primers specific to the transgene sequence (Fig. 6A). Northern blotting of t-siRNAs derived from the hairpin transgene revealed the accumulation of 21-, 22- and 24-nt t-siRNAs, similar to that observed in RdRp-transgenic *N. benthamiana* plants (Fig. 6B), which, based on our hypothesis, should provide immunity to systemic CYSDV infection.

To test this, both transgenic and non-transgenic melon plants were inoculated at the one true leaf stage by CYSDV viruliferous
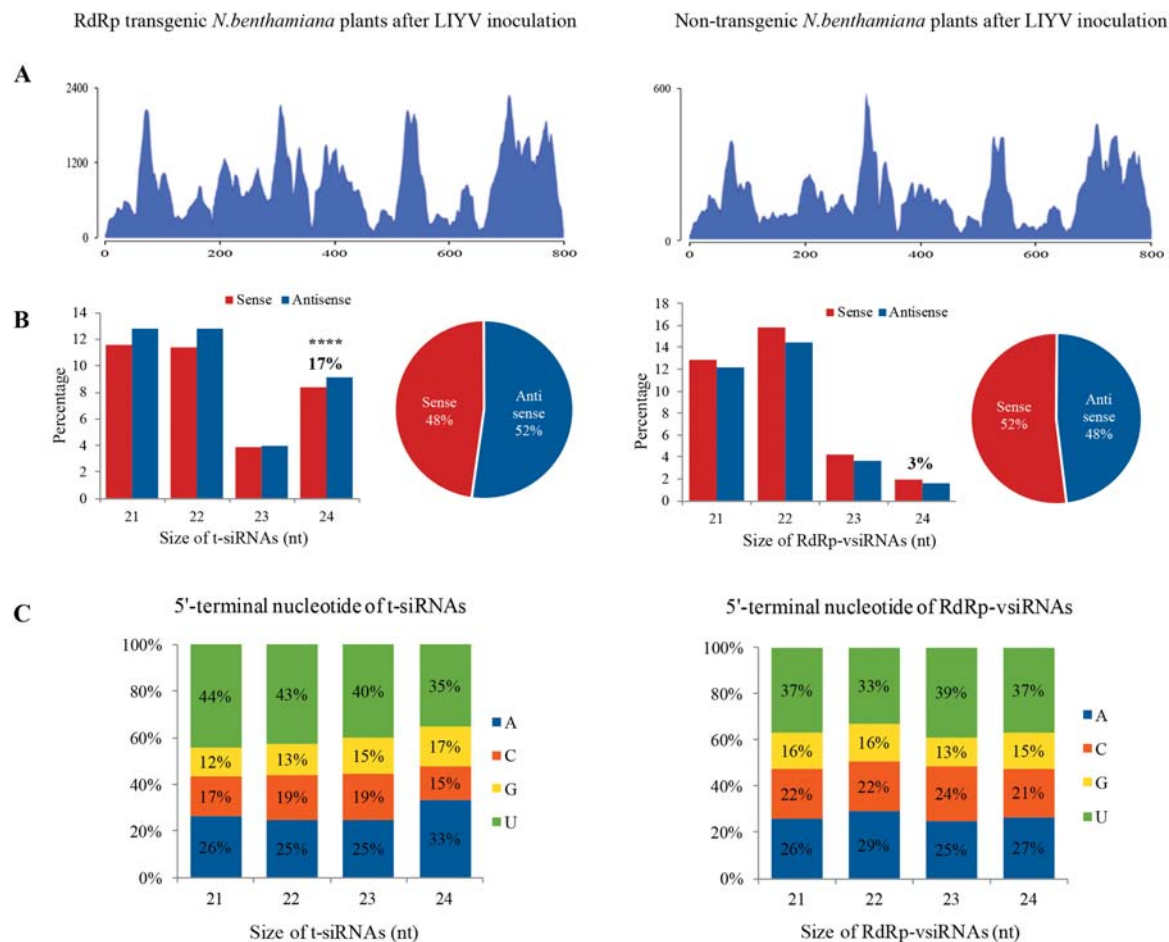
RdRp transgenic *N. benthamiana* plants after LIYV inoculation

Non-transgenic *N. benthamiana* plants after LIYV inoculation

Fig. 5 Characterization and comparison of 21–24-nucleotide (nt) transgene-derived small interfering RNAs (t-siRNAs) (left) and virus-derived small interfering RNAs (vsiRNAs) (right) mapped to the 801-nt RNA-dependent RNA polymerase (RdRp) transgene in transgenic and non-transgenic *Nicotiana benthamiana* plants after *Lettuce infectious yellows virus* (LIYV) inoculation. (A) Sequence distribution of t-siRNAs and RdRp-vsiRNAs. Note that the scale used for the transgenic plants is different from that used for the non-transgenic, LIYV-infected plants. The graphs were generated with t-siRNAs and RdRp-vsiRNAs from library 10 (RdRp-TG-1) and library 4 (Non-TG-1) using CLC genomics workbench; other biological replicates displaying a similar pattern can be seen in Fig. S3 (see Supporting Information). (B) Size distribution of t-siRNAs and RdRp-vsiRNAs. Histograms show the read percentages for each size class for the sense (red) and antisense (blue) orientations. The statistical significance of the difference between the 24-nt t-siRNA and RdRp-vsiRNA populations in three biological replicates was calculated; two-tailed *t*-test: ****$P < 0.0001$. The percentage of the 21–24-nt sense and antisense reads in total is shown within the pie graph. (C) Relative frequency of 5′-terminal nucleotides in t-siRNAs and RdRp-vsiRNAs.

B. tabaci, as no agroinoculation system is available for CYSDV. In two independent trials, all non-transgenic melon plants (17/17) inoculated with CYSDV developed stunting and yellowing symptoms similar to those on plants infected by LIYV, and no symptoms were observed on any of the inoculated PRO-transgenic melon plants (30/30) (Fig. 6C; Table 3). The systemic infection in non-transgenic control plants was confirmed by RT-PCR using CYSDV CP specific primers, but no product was obtained from the transgenic plants (Fig. 6D); this shows the immunity of the PRO-transgenic melon plants to systemic CYSDV infection, as predicted.

DISCUSSION

RNA silencing-mediated transgenic plants have been shown to confer high levels of resistance against many plant viruses, but, so far, only limited success has been achieved for viruses in the family *Closteroviridae*. Several efforts have been made to develop transgenic plants resistant to *Citrus tristeza virus* (CTV, *Closterovirus*) and SPCSV (*Crinivirus*). Transgenic lines of Mexican lime plants expressing complete and truncated versions of CTV P23 or P25 genes, the 3′-terminal 549 nt of the CTV gRNA in sense, antisense and intron-hairpin formats, as well as a hairpin construct
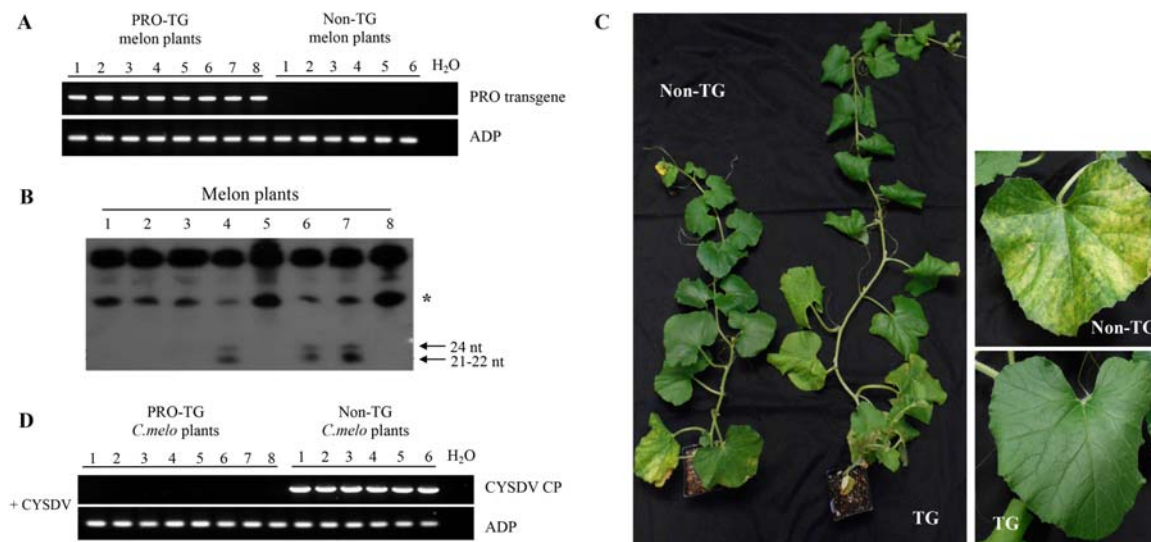
Fig. 6 Molecular characterization and resistance examination of transgenic melon plants. (A) Transgene expression in melon [papain-like cysteine proteinase-transgenic (PRO-TG)] plants was examined by reverse transcription-polymerase chain reaction (RT-PCR). Non-transgenic (Non-TG) plants were used as control. RT-PCR was performed using primers corresponding to the PRO transgene. The same RNA samples were used to amplify the ADP (ADP-ribosylation factor-like) gene as reference control for melon plants. (B) Northern blot analysis of the transgene sequence-derived small RNAs in healthy transgenic and non-transgenic melon plants. Lanes 1, 2, 3, 5, 8, healthy, non-transgenic plants; lanes 4, 6, 7, healthy, transgenic plants. A cross-reacting band (asterisk) was used as a loading control. (C) Response of non-transgenic (Non-TG) and transgenic (TG) melon plants to *Cucurbit yellow stunting disorder virus* (CYSDV) inoculation. Symptoms were observed at 4 weeks post-inoculation. (D) RT-PCR was performed using total RNA extracted from TG and non-TG melon plants that had been inoculated with CYSDV; primers corresponding to the coat protein (CP) were applied. The same RNA samples were used to amplify the ADP genes as reference control for melon plants.

carrying full-length, untranslatable versions of the CTV P25, P20 and P23 genes have been developed (Domínguez *et al.*, 2002a,b; Fagoaga *et al.*, 2006; López *et al.*, 2010; Soler *et al.*, 2012). Only the last construct that contains all three genes coding for the silencing suppressors of CTV conferred complete resistance to the virus, whereas the others showed only partial resistance or remained susceptible to CTV. SPCSV is a very economically important crinivirus, and transgenic sweet potatoes harbouring the gene fragments of SPCSV RdRp and CP have been developed, but displayed only partial resistance to SPCSV (Kreuze *et al.*, 2008; Sivparsad and Gubba, 2014). The mechanisms behind the varying levels of resistance caused by different viral sequences are unknown, but possibly may be caused by the lesser effects of these sequences on virus accumulation when targeted by the RNAi machinery. Therefore, from lessons learnt from previous

Table 3 Numbers of non-transgenic (Non-TG) and papain-like cysteine proteinase-transgenic (PRO-TG) melon plants showing *Cucurbit yellow stunting disorder virus* (CYSDV) symptoms recorded at 4 weeks post-inoculation.

CYSDV challenge	Non-TG *Cucumis melo* Whitefly	PRO-TG *Cucumis melo* Whitefly
Trial 1	10/10	0/17
Trial 2	7/7	0/13
Total	17/17	0/30

failed attempts in our own laboratory to develop immunity against LIYV using sequences from RNA2, we decided to target virus-derived sequences from the viral replicase-encoding region on RNA1 of criniviruses (Kiss, 2013). In this study, RdRp-transgenic *N. benthamiana* and PRO-transgenic melon plants immune to systemic LIYV and CYSDV infection, respectively, were characterized. Although a 479-nt RdRp fragment of SPCSV derived from the second half of the full-length ORF was studied and showed weak effects, the 801-nt RdRp transgene of the LIYV-immune *N. benthamiana* plants chosen is from another portion of the homologous RdRp gene of LIYV. Whether similar gene segments of different criniviruses would also confer high levels of resistance transformed to their host plants requires further investigation. Moreover, the 801-nt LIYV RdRp transgene sequence exhibited 68% and 64% identity with the corresponding regions of the *Tomato infectious chlorosis virus* (TICV) and *Beet pseudoyellows virus* (BPYV) genomes. Considering the conserved genomic structure and similar functional properties of the homologous proteins produced in the genus *Crinivirus*, our study could have immediate translational applications for the control of diseases caused by other economically important criniviruses.

Interestingly, the accumulation of 24-nt t-siRNAs was detected by northern blotting in LIYV immune-transgenic *N. benthamiana*, but not in other previously reported transgenic plants that remained susceptible or exhibited partial resistance to their

cognate criniviruses. For instance, northern blot analysis of transgenic *N. benthamiana* containing the HEL gene construct of LIYV, and transgenic sweet potato plants comprising the RdRp gene of SPCSV, showed large amounts of 21- and 22-nt t-siRNAs, whereas, in the PRO-transgenic *N. benthamiana* plants mentioned above that showed immunity to LIYV only in the early generations, the elevated level of 24-nt t-siRNAs was observed (Kiss, 2013; Kreuze *et al.*, 2008). We hypothesize that the accumulation of 24-nt t-siRNAs is associated with crinivirus immunity.

Illumina sequencing was applied in our attempts to explore the RNA-based antiviral mechanisms during crinivirus–host plant interactions and to characterize the t-siRNAs that confer full resistance. For the first time, the vsiRNAs generated on crinivirus infection were characterized. Bioinformatic analysis of the deep sequencing data revealed that LIYV infection triggered the production of small amounts of vsiRNAs relative to many other virus–host combinations (Donaire *et al.*, 2009; Xia *et al.*, 2014), accounting for only 5.73% of the total 18–30-nt reads. This is probably a result of the low virus accumulation rates of criniviruses in their host plants. In general, DCL4-dependent 21-nt vsiRNAs are the most abundant species, followed by 22-nt vsiRNAs generated by DCL2 in a redundant and hierarchical manner (Blevins *et al.*, 2006; Bouché *et al.*, 2006; Deleris *et al.*, 2006). However, LIYV-derived siRNAs of 22 nt (29%) were more abundant than those of 21 nt (23%) (Fig. 3B), similar to that observed in *Tobacco rattle virus* (TRV)-infected *N. benthamiana* and *Cotton leafroll dwarf virus* (CLRDV)-infected cotton plants (Donaire *et al.*, 2008; Silva *et al.*, 2011), suggesting different biosynthetic pathways in different virus–host pathosystems. Somewhat surprisingly, the amount of LIYV RNA2-specific vsiRNAs was threefold higher than that of RNA1. This might be explained by the higher replication rate of RNA2, which produces several subgenomic RNAs and defective RNAs, thus generating more abundant dsRNA replication intermediates for dicing, or by some unknown host defence and pathogen counter-defence mechanism with less targeting of viral replicase complexes, thus facilitating successful virus infection. In *A. thaliana*, AGO1 and AGO2 have been shown to play important antiviral roles and bind small RNAs with 5′-terminal U and A, respectively (Mi *et al.*, 2008). We also observed a greater prevalence of U and A at the 5′-termini of LIYV-derived vsiRNAs, showing the considerable conservation of parts of the RNA silencing machinery (Matzke *et al.*, 2001; Waterhouse *et al.*, 2001).

To characterize t-siRNAs that are associated with LIYV immunity, we compared the biogenesis, composition and abundance of 801-nt RdRp sequence-derived t-siRNAs and vsiRNAs. Nearly the same patterns were obtained when characterizing t-siRNA populations in RdRp-transgenic *N. benthamiana* plants before and after virus inoculation, except that twice as many reads were counted in the plants after inoculation, indicating the activation of the antiviral defences derived from the transgene. Interestingly, when comparing t-siRNAs with RdRp-vsiRNAs, their sequence distribution and 5′-terminal nucleotides also exhibited very similar patterns, reflecting a sequence bias for the generation of siRNAs. However, the size distribution analysis of t-siRNAs and RdRp-vsiRNAs of 21–24 nt in length, as well as the northern blot results, revealed a greater abundance of 24-nt t-siRNAs in transgenic plants, indicating the activation of DCL3 in t-siRNA processing, in addition to the cooperative interaction between DCL2 and DCL4.

To further test our hypothesis of the correlation of accumulated 24-nt t-siRNAs with crinivirus immunity in another crinivirus–host system, transgenic melon plants transformed with a hairpin construct of the CYSDV PRO gene sequence, and which showed immunity to systemic CYSDV infection, were developed. As predicted, the accumulation of 24-nt t-siRNAs was detected in these plants by northern blotting, thus supporting our hypothesis. To date, the roles of DCL3-dependent 24-nt siRNAs in antiviral defence against RNA viruses in plants have remained unclear (Andika *et al.*, 2015), and questions arising from this study, such as how the expression level of 24-nt t-siRNAs is regulated and their roles in RNA silencing-mediated viral immunity, need to be further investigated. Our study helps to fill in the blank areas of the study of criniviruses and provides a first step towards an understanding of RNA-based antiviral immunity and counter-defence in crinivirus–host interactions.

EXPERIMENTAL PROCEDURES

Molecular cloning and generation of transgenic plants

Transgenic plants were generated as described previously (Kiss, 2013). In brief, an 801-nt fragment of the RdRp gene of LIYV (position 5918–6718 nt of the LIYV RNA1 genome; Accession number NC_003617.1) was amplified from an infectious clone pJW100 by PCR (Wang *et al.*, 2009). A 346-nt fragment of the PRO encoding sequence of CYSDV (position 101–446 nt of the CYSDV RNA1 genome; Accession number NC_004809.1) was amplified from CYSDV-infected melon plant leaf tissue by RT-PCR. The PCR products were cloned into the TA-cloning vector pCR™8/GW/TOPO (Invitrogen Corporation, Carlsbad, CA, USA), and subsequently transferred into the binary vector pCB2004B (Lei *et al.*, 2007) using the Gateway cloning system following the manufacturer's instructions (Invitrogen Corporation). The primers used for cloning are listed in Table S2 (see Supporting Information). The constructed binary vectors were introduced into *Agrobacterium tumefaciens* LBA4404 by electroporation and selected to generate transgenic *N. benthamiana* and melon plants at the Ralph M. Parsons Foundation Plant Transformation Facility (University of California, Davis, CA, USA).

Screening of transgenic plants

The T_0 plants obtained were checked for the presence of the LIYV RdRp and CYSDV PRO transgenes by PCR with total genomic DNA extracted using the method of Dellaporta *et al.* (1983); primers for transgene cloning were used (Table S2). Seeds were collected from positive plants, and the T_1 generation was screened by germinating seeds on KCMS medium

(4.32 g/L MS salt, 7 g/L phytoagar, 10 ml/L vitamin solution (100×), pH5.7) containing ammonium glufosinate (50 mg/L) and by PCR as for the T_0 plants. Positive plants were transplanted to soil and used for subsequent experiments and T_2 seed collection.

Virus inoculation and symptom evaluation

Transgenic and non-transgenic *N. benthamiana* plants were challenged with LIYV by whitefly transmission and agroinoculation at the four- to six-leaf stages in separate experiments. LIYV was maintained in *Chenopodium murale* and lettuce (*Lactuca sativa*, cv. Summer Bibb) plants by transmission using the whitefly *B. tabaci*. Non-viruliferous whiteflies reared on lima bean (*Phaseolus limensis*) plants were collected and allowed an acquisition access period (AAP) of at least 24 h on LIYV-infected *C. murale* or lettuce plants, following which whiteflies were transferred to *N. benthamiana* plants as described previously (Tian *et al.*, 1996). Whiteflies were sprayed after a 3-day inoculation access period. Agroinfiltration of LIYV for systemic infection was performed following the protocol described by Lindbo (2007). After treatment, *N. benthamiana* plants were kept in a glasshouse at 20–25 °C with a 14-h light period for symptom development and evaluation.

CYSDV is classified as a restricted pathogen in California, and was maintained in squash plants with viruliferous *B. tabaci* in the Biosafety Level 3-P Contained Research Facility (CRF, University of California, Davis, CA, USA). Transgenic and non-transgenic melon plants were inoculated by maintaining plants at the one true leaf stage in a large cage containing a CYSDV squash plant that was colonized by *B. tabaci*. After a 1-week exposure to viruliferous *B. tabaci*, melon plants were sprayed and moved into the glasshouse.

Total RNA extraction and RT-PCR

Transgenic plants were tested using RT-PCR for the presence of transgene-derived RNA. Total RNA was extracted from plant leaf tissues at the four- to six-leaf stages before virus inoculation with TRIzol Reagent (Invitrogen Corporation). RT-PCR was conducted in two steps: cDNA synthesis using SuperScript™ II Reverse Transcriptase (Invitrogen Corporation) with random primer, followed by PCR amplification using GoTaq® Flexi DNA Polymerase (Promega Corporation, Madison, WI, USA) with LIYV RdRp and CYSDV PRO transgene cloning primers.

Transgenic and non-transgenic *N. benthamiana* and melon plants at 3–4 wpi were tested for LIYV and CYSDV by RT-PCR. Primers flanking the LIYV CP (530 bp) and CYSDV CP (761 bp) genes were used. PP2A (protein phosphatase) of *N. benthamiana* and ADP (ADP-ribosylation factor-like) of *C. melo* were used as control RNAs. All primer sequences can be found in Table S2.

Small RNA polyethylene glycol (PEG) fractionation and northern blot analysis

To enrich the samples for small RNAs, we used the PEG-NaCl method described previously (Wuriyanghan and Falk, 2013). In brief, total RNA was isolated from the plant samples using Trizol reagent and large RNAs were precipitated using 1 M NaCl and 10% PEG 8000 by 30 min of incubation on ice and centrifugation at 12 000 g for 20 min at 4°C. Small RNAs were recovered from the supernatant using three volumes of cold ethanol

at −20°C overnight. The pellet was collected by centrifugation at 12 000 g for 20 min at 4°C and resuspended with RNAse-free water.

Small RNA hybridization was performed according to the method described previously (Wuriyanghan *et al.*, 2011). The transgene sequences were amplified by PCR and used to make probes for the LIYV RdRp and CYSDV PRO sequences. The forward primers were designed containing the T7 promoter sequence (in italic): T7_LIYV RdRp-F, 5′-*TAATACGACT CACTATAGG*GAGCAAGTCCAAACCATACCAC-3′; T7_CYSDV PRO-F, 5′-*TAATACGACTCACTATAGG*GTCGTCACTAGTTGCCGCTGAC-3′. PCR products were purified and ^{32}P-UTP-labelled negative strand LIYV RdRp and CYSDV PRO transcripts were generated *in vitro* using the T7 Maxiscript Kit (Ambion Inc., Austin, TX, USA) following the manufacturer's instructions. The fragments were purified using NucAway Spin Columns (Ambion Inc.), fragmented in 120 mM Na_2CO_3 : 80 mM $NaHCO_3$ solution at 65 °C for 30 min and used as probes for hybridization.

Deep sequencing and bioinformatic analysis of small RNA sequences

Small RNAs were extracted from the upper non-inoculated leaves of the same transgenic and non-transgenic *N. benthamiana* plants before and 3 weeks after LIYV inoculation; triplicate biological replicates, i.e. small RNA samples from three transgenic and three non-transgenic *N. benthamiana* plants, were prepared and sent to Beijing Genomics Institute (BGI, Philadelphia, PA, USA) for library construction and sequencing. A total of 12 small RNA libraries were sequenced using an Illumina Hiseq4000 system in one lane. Raw data were obtained after adapter trimming and cleaning of the reads; data analysis was performed using the CLC Genomics Workbench program (QIAGEN, Hilden, Germany), Galaxy (https://usegalaxy. org) and R code/package viRome (http://sourceforge.net/projects/ virome).

REFERENCES

Abrahamian, P.E. and Abou-Jawdah, Y. (2014) Whitefly-transmitted criniviruses of cucurbits: current status and future prospects. *Virus Dis.* **25**, 26–38.

Aguilar, J.M., Abad, J. and Aranda, M.A. (2006) Resistance to Cucurbit yellow stunting disorder virus in cucumber. *Plant Dis.* **90**, 583–586.

Aliyari, R., Wu, Q., Li, H.-W., Wang, X.-H., Li, F., Green, L.D., Han, C.S., Li, W.-X. and Ding, S.-W. (2008) Mechanism of induction and suppression of antiviral immunity directed by virus-derived small RNAs in Drosophila. *Cell Host Microbe*, **4**, 387–397.

Andika, I.B., Maruyama, K., Sun, L., Kondo, H., Tamada, T. and Suzuki, N. (2015) Different Dicer-like protein components required for intracellular and systemic antiviral silencing in *Arabidopsis thaliana*. *Plant Signal. Behav.* **10**, e1039214.

Blevins, T., Rajeswaran, R., Shivaprasad, P.V., Beknazariants, D., Si-Ammour, A., Park, H.-S., Vazquez, F., Robertson, D., Meins, F., Hohn, T. and Pooggin, M.M. (2006) Four plant Dicers mediate viral small RNA biogenesis and DNA virus induced silencing. *Nucleic Acids Res.* **34**, 6233–6246.

Borges, F. and Martienssen, R.A. (2015) The expanding world of small RNAs in plants. *Nat. Rev. Mol. Cell Biol.* **16**, 727.

Bouché, N., Lauressergues, D., Gasciolli, V. and Vaucheret, H. (2006) An antagonistic function for Arabidopsis DCL2 in development and a new function for DCL4 in generating viral siRNAs. *EMBO J.* **25**, 3347–3356.

Brodersen, P., Sakvarelidze-Achard, L., Bruun-Rasmussen, M., Dunoyer, P., Yamamoto, Y.Y., Sieburth, L. and Voinnet, O. (2008) Widespread translational inhibition by plant miRNAs and siRNAs. *Science*, **320**, 1185–1190.

Carbonell, A. and Carrington, J.C. (2015) Antiviral roles of plant ARGONAUTES. *Curr. Opin. Plant Biol.* **27**, 111–117.

Deleris, A., Gallego-Bartolome, J., Bao, J., Kasschau, K.D., Carrington, J.C. and Voinnet, O. (2006) Hierarchical action and inhibition of plant Dicer-like proteins in antiviral defense. *Science*, **313**, 68–71.

Dellaporta, S.L., Wood, J. and Hicks, J.B. (1983) A plant DNA minipreparation: version II. *Plant Mol. Biol. Rep.* **1**, 19–21.

Diaz-Pendon, J.A., Li, F., Li, W.-X. and Ding, S.-W. (2007) Suppression of antiviral silencing by cucumber mosaic virus 2b protein in Arabidopsis is associated with drastically reduced accumulation of three classes of viral small interfering RNAs. *Plant Cell*, **19**, 2053–2063.

Ding, S.-W. (2010) RNA-based antiviral immunity. *Nat. Rev. Immunol.* **10**, 632.

Ding, S.-W. and Voinnet, O. (2007) Antiviral immunity directed by small RNAs. *Cell*, **130**, 413–426.

Domínguez, A., de Mendoza, A.H., Guerri, J., Cambra, M., Navarro, L., Moreno, P. and Peña, L. (2002a) Pathogen-derived resistance to *Citrus tristeza virus* (CTV) in transgenic Mexican lime (*Citrus aurantifolia* (Christ.) Swing.) plants expressing its *p25* coat protein gene. *Mol. Breed.* **10**, 1–10.

Domínguez, A., Fagoaga, C., Navarro, L., Moreno, P. and Pena, L. (2002b) Constitutive expression of untranslatable versions of the p25 coat protein gene in Mexican lime (*Citrus aurantifolia* (Christm.) Swing.) transgenic plants does not confer resistance to *Citrus tristeza* virus (CTV). In: *Proceedings of the XV Conference of the International Organization of Citrus Virologists*, pp. 341–344. Riverside, CA: University of California.

Donaire, L., Barajas, D., Martinez-Garcia, B., Martinez-Priego, L., Pagan, I. and Llave, C. (2008) Structural and genetic requirements for the biogenesis of tobacco rattle virus-derived small interfering RNAs. *J. Virol.* **82**, 5167–5177.

Donaire, L., Wang, Y., Gonzalez-Ibeas, D., Mayer, K.F., Aranda, M.A. and Llave, C. (2009) Deep-sequencing of plant viral small RNAs reveals effective and widespread targeting of viral genomes. *Virology*, **392**, 203–214.

Fagoaga, C., López, C., de Mendoza, A.H., Moreno, P., Navarro, L., Flores, R. and Peña, L. (2006) Post-transcriptional gene silencing of the p23 silencing suppressor of *Citrus tristeza* virus confers resistance to the virus in transgenic Mexican lime. *Plant Mol. Biol.* **60**, 153–165.

Garcia-Ruiz, H., Takeda, A., Chapman, E.J., Sullivan, C.M., Fahlgren, N., Brempelis, K.J. and Carrington, J.C. (2010) Arabidopsis RNA-dependent RNA polymerases and dicer-like proteins in antiviral defense and small interfering RNA biogenesis during Turnip Mosaic Virus infection. *Plant Cell*, **22**, 481–496.

Helliwell, C.A. and Waterhouse, P.M. (2005) Constructs and methods for hairpin RNA-mediated gene silencing in plants. *Methods Enzymol.* **392**, 24–35.

Kiss, Z.A. (2013) *Functional Investigations of the Lettuce Infectious Yellow Virus (LIYV)-Encoded Proteins, P34, P5, P9 and the Development of LIYV and Cucurbit Yellow Stunting Disorder Virus (CYSDV) Immunity Using RNA Interference.* Davis, CA: University of California. Available at https://search.proquest.com/docview/1519305574?accountid=14505.

Kiss, Z.A., Medina, V. and Falk, B.W. (2013) Crinivirus replication and host interactions. *Front. Microbiol.* **4**, 99.

Kreuze, J.F., Klein, I.S., Lazaro, M.U., Chuquiyuri, W.J., Morgan, G.L., Mejía, P.G., Ghislain, M. and Valkonen, J.P. (2008) RNA silencing-mediated resistance to a crinivirus (Closteroviridae) in cultivated sweetpotato (*Ipomoea batatas* L.) and development of sweetpotato virus disease following co-infection with a potyvirus. *Mol. Plant Pathol.* **9**, 589–598.

Langmead, B. and Salzberg, S.L. (2012) Fast gapped-read alignment with Bowtie 2. *Nat. Methods*, **9**, 357–359.

Lei, Z.-Y., Zhao, P., Cao, M.-J., Cui, R., Chen, X., Xiong, L.-Z., Zhang, Q.-F., Oliver, D.J. and Xiang, C.-B. (2007) High-throughput binary vectors for plant gene function analysis. *J. Integr. Plant Biol.* **49**, 556–567.

Lindbo, J.A. (2007) High-efficiency protein expression in plants from agroinfection-compatible Tobacco mosaic virus expression vectors. *BMC Biotechnol.* **7**, 52.

López, C., Cervera, M., Fagoaga, C., Moreno, P., Navarro, L., Flores, R. and Peña, L. (2010) Accumulation of transgene-derived siRNAs is not sufficient for RNAi-mediated protection against *Citrus tristeza* virus in transgenic Mexican lime. *Mol. Plant Pathol.* **11**, 33–41.

Marco, C.F., Aguilar, J.M., Abad, J., Gómez-Guillamón, M.L. and Aranda, M.A. (2003) Melon resistance to Cucurbit yellow stunting disorder virus is characterized by reduced virus accumulation. *Phytopathology*, **93**, 844–852.

Matzke, M.A. and Birchler, J.A. (2005) RNAi-mediated pathways in the nucleus. *Nat. Rev. Genet.* **6**, 24–35.

Matzke, M.A., Matzke, A.J., Pruss, G.J. and Vance, V.B. (2001) RNA-based silencing strategies in plants. *Curr. Opin. Genet. Dev.* **11**, 221–227.

McCreight, J.D. and Wintermantel, W.M. (2011) Genetic resistance in melon PI 313970 to Cucurbit yellow stunting disorder virus. *HortScience*, **46**, 1582–1587.

Mi, S., Cai, T., Hu, Y., Chen, Y., Hodges, E., Ni, F., Wu, L., Li, S., Zhou, H., Long, C., Chen, S., Hannon, G.J. and Qi, Y. (2008) Sorting of small RNAs into *Arabidopsis* argonaute complexes is directed by the 5′ terminal nucleotide. *Cell*, **133**, 116–127.

Odokonyero, D., Mendoza, M.R., Moffett, P. and Scholthof, H.B. (2017) Tobacco rattle virus (TRV)-mediated silencing of *Nicotiana benthamiana* ARGONAUTES (NbAGOs) reveals new antiviral candidates and dominant effects of TRV-NbAGO1. *Phytopathology*, **107**, 977–987.

Ogwok, E., Ilyas, M., Alicai, T., Rey, M.E. and Taylor, N.J. (2016) Comparative analysis of virus-derived small RNAs within cassava (*Manihot esculenta Crantz*) infected with cassava brown streak viruses. *Virus Res.* **215**, 1–11.

Okuda, S., Okuda, M., Sugiyama, M., Sakata, Y., Takeshita, M. and Iwai, H. (2013) Resistance in melon to Cucurbit chlorotic yellows virus, a whitefly-transmitted crinivirus. *Eur. J. Plant Pathol.* **135**, 313–321.

Pantaleo, V., Saldarelli, P., Miozzi, L., Giampetruzzi, A., Gisel, A., Moxon, S., Dalmay, T., Bisztray, G. and Burgyan, J. (2010) Deep sequencing analysis of viral short RNAs from an infected Pinot Noir grapevine. *Virology*, **408**, 49–56.

Park, S.O., Crosby, K.M. and Mirkov, T.E. (2006) Detection of loci for cucurbit yellow stunting disorder virus resistance in *Cucumis melo* L. In: *XXVII International Horticultural Congress-IHC2006: International Symposium on Structural and Functional Genomics of 763*, (Drew R., ed), pp. 207–214. Proc. XXVII IHC-S7 Struct. and Funct. Genomics of Hort. Plants, Acta Hort. 763, ISHS 2007.

Prins, M., Laimer, M., Noris, E., Schubert, J., Wassenegger, M. and Tepfer, M. (2008) Strategies for antiviral resistance in transgenic plants. *Mol. Plant Pathol.* **9**, 73–83.

Pumplin, N. and Voinnet, O. (2013) RNA silencing suppression by plant pathogens: defence, counter-defence and counter-counter-defence. *Nat. Rev. Microbiol.* **11**, 745.

Silva, T.F., Romanel, E.A., Andrade, R.R., Farinelli, L., Østerås, M., Deluen, C., Corrêa, R.L., Schrago, C.E. and Vaslin, M.F. (2011) Profile of small interfering RNAs from cotton plants infected with the polerovirus Cotton leafroll dwarf virus. *BMC Mol. Biol.* **12**, 40.

Simón-Mateo, C. and García, J.A. (2011) Antiviral strategies in plants based on RNA silencing. *Biochim. Biophys. Acta*, **1809**, 722–731.

Sivparsad, B. and Gubba, A. (2014) Development of transgenic sweet potato with multiple virus resistance in South Africa (SA). *Transgenic Res.* **23**, 377–388.

Smith, N.A., Singh, S.P., Wang, M.-B., Stoutjesdijk, P.A., Green, A.G. and Waterhouse, P.M. (2000) Gene expression: total silencing by intron-spliced hairpin RNAs. *Nature*, **407**, 319–320.

Soler, N., Plomer, M., Fagoaga, C., Moreno, P., Navarro, L., Flores, R. and Peña, L. (2012) Transformation of Mexican lime with an intron-hairpin construct expressing untranslatable versions of the genes coding for the three silencing suppressors of *Citrus tristeza* virus confers complete resistance to the virus. *Plant Biotechnol. J.* **10**, 597–608.

Stewart, L.R., Medina, V., Tian, T., Turina, M., Falk, B.W. and Ng, J.C. (2010) A mutation in the Lettuce infectious yellows virus minor coat protein disrupts whitefly transmission but not in planta systemic movement. *J. Virol.* **84**, 12 165–12 173.

Tian, T., Klaassen, V., Soong, J., Wisler, G., Duffus, J. and Falk, B. (1996) Generation of cDNAs specific to lettuce infectious yellows closterovirus and other whitefly-transmitted viruses by RT-PCR and degenerate oligonucleotide primers corresponding to the closterovirus gene encoding the heat shock protein 70 homolog. *Phytopathology*, **86**, 1167–1173.

Tian, T., Rubio, L., Yeh, H.H., Crawford, B. and Falk, B.W. (1999) Lettuce infectious yellows virus: in vitro acquisition analysis using partially purified virions and the whitefly *Bemisia tabaci*. *J. Gen. Virol.* **80**, 1111–1117.

Tzanetakis, I.E., Martin, R.R. and Wintermantel, W.M. (2013) Epidemiology of criniviruses: an emerging problem in world agriculture. *Front. Microbiol.* **4**, 119.

Wang, J., Turina, M., Stewart, L.R., Lindbo, J.A. and Falk, B.W. (2009) Agroinoculation of the Crinivirus, Lettuce infectious yellows virus, for systemic plant infection. *Virology*, **392**, 131–136.

Wassenegger, M. and Krczal, G. (2006) Nomenclature and functions of RNA-directed RNA polymerases. *Trends Plant Sci.* **11**, 142–151.

Waterhouse, P.M., Wang, M.-B. and Lough, T. (2001) Gene silencing as an adaptive defence against viruses. *Nature*, **411**, 834–842.

Wuriyanghan, H. and Falk, B.W. (2013) RNA interference towards the potato psyllid, *Bactericera cockerelli*, is induced in plants infected with recombinant tobacco mosaic virus (TMV). *PLoS One*, **8**, e66050.

Wuriyanghan, H., Rosa, C. and Falk, B.W. (2011) Oral delivery of double-stranded RNAs and siRNAs induces RNAi effects in the potato/tomato psyllid, *Bactericera cockerelli*. *PLoS One*, **6**, e27736.

Xia, Z., Peng, J., Li, Y., Chen, L., Li, S., Zhou, T. and Fan, Z. (2014) Characterization of small interfering RNAs derived from Sugarcane mosaic virus in infected maize plants by deep sequencing. *PLoS One*, **9**, e97013.

Yeh, H.H., Tian, T., Rubio, L., Crawford, B. and Falk, B.W. (2000) Asynchronous accumulation of lettuce infectious yellows virus RNAs 1 and 2 and identification of an RNA 1 trans enhancer of RNA 2 accumulation. *J. Virol.* **74**, 5762–5768.

SUPPORTING INFORMATION

Additional supporting information may be found in the online version of this article at the publisher's web-site.

Table S1 Detailed data analysis on individual libraries.

Table S2 Primer sequences used for the cloning of transgenes and testing of viral infection. The accession numbers of the target genes are listed.

Fig. S1 Single-nucleotide resolution maps of virus-derived small interfering RNAs (vsiRNAs) from libraries of two other biological replicates (Non-TG-2 and Non-TG-3) along the *Lettuce infectious yellows virus* (LIYV) genome in both positive (red) and negative (blue) polarity.

Fig. S2 Characterization of 21–24-nucleotide (nt) transgene-derived small interfering RNAs (t-siRNAs) in transgenic *Nicotiana benthamiana* plants before *Lettuce infectious yellows virus* (LIYV) inoculation. (A) Sequence distribution of t-siRNAs. The graphs were generated with t-siRNAs from library 7 (RdRp-TG-1) using the CLC genomics workbench program; the other biological replicates displayed a similar pattern and can be seen in Fig. S3 (see Supporting Information). (B) Size distribution of t-siRNAs. Histograms show read percentages for each size class for the sense (red) and antisense (blue) orientations. The statistical significance of the difference between the t-siRNA and RNA-dependent RNA polymerase-virus-derived small interfering RNA (RdRp-vsiRNA) populations in three biological replicates was calculated; two-tailed *t*-test. Only 24-nt siRNAs showed a significant difference: ****$P < 0.0001$. The percentage of the 21–24-nt sense and antisense reads in total is shown within the pie graph. (C) Relative frequency of 5′-terminal nucleotides in t-siRNAs and RdRp-vsiRNAs.

Fig. S3 Sequence distribution of transgene-derived small interfering RNAs (t-siRNAs) and virus-derived small interfering RNAs (vsiRNAs) from libraries of two other biological replicates that mapped to the 801-nucleotide RNA-dependent RNA polymerase (RdRp) transgene in transgenic and non-transgenic *Nicotiana benthamiana* plants. Note that the scale is different based on the amount of reads in each library.